HHS Public Access

Author manuscript

J Immunol. Author manuscript; available in PMC 2017 January 01.

Published in final edited form as:

J Immunol. 2016 January 1; 196(1): 336–344. doi:10.4049/jimmunol.1502037.

Zinc and Manganese Chelation by Neutrophil S100A8/A9 (Calprotectin) Limits Extracellular *Aspergillus fumigatus* Hyphal Growth and Corneal Infection

Heather L. Clark[*,†], **Anupam Jhingran**[‡], **Yan Sun**[*], **Chairut Vareechon**[*], **Steven de Jesus Carrion**[*], **Eric P. Skaar**[§,#], **Walter J. Chazin**[¶,‖], **Jose Antonio Calera**[**], **Tobias M. Hohl**[‡], and **Eric Pearlman**[*,†]

[*]Department of Ophthalmology and Visual Science, Case Western Reserve University, Cleveland OH.

[†]Departments of Ophthalmology and Physiology and Biophysics, University of California, Irvine CA.

[‡]Infectious Disease Service, Department of Medicine, Memorial Sloan-Kettering Cancer Center, New York, NY.

[§]Department of Pathology, Microbiology & Immunology, Nashville, TN.

[¶]Department of Biochemistry, Nashville, TN.

[‖]Center for Structural Biology, Vanderbilt University School of Medicine, Nashville, TN.

[#]Veterans Affairs Tennessee Valley Healthcare System.

[**]Instituto de Biología Funcional y Genómica (IBFG), Centro Mixto del Consejo Superior de Investigaciones Científicas y Universidad de Salamanca, Salamanca, Spain. 1.

Abstract

Calprotectin, a heterodimer of S100A8 and S100A9, is an abundant neutrophil protein which possesses anti-microbial activity primarily due to its ability to chelate zinc and manganese. In the current study, we showed that neutrophils from calprotectin-deficient S100A9 $^{-/-}$ mice have an impaired ability to inhibit *Aspergillus fumigatus* hyphal growth *in vitro*, and in infected corneas in a murine model of fungal keratitis; however, the ability to inhibit hyphal growth was restored in S100A9$^{-/-}$ mice by injecting recombinant calprotectin. Further, using recombinant calprotectin with mutations in either the Zn and Mn binding sites or the Mn binding site alone, we show that both zinc and manganese binding are necessary for calprotectin's anti-hyphal activity. In contrast to hyphae, we found no role for neutrophil calprotectin in uptake or killing of intracellular *A. fumigatus* conidia either *in vitro*, or in a murine model of pulmonary aspergillosis. We also found that an *A. fumigatus* Δ*zafA* mutant, which demonstrates deficient zinc transport, exhibits impaired growth in infected corneas and following incubation with neutrophils or calprotectin *in vitro* as compared to wild-type. Collectively, these studies demonstrate a novel stage - specific susceptibility of *A. fumigatus* to zinc and manganese chelation by neutrophil-derived calprotectin.

Correspondence: Eric Pearlman. epearlma@uci.edu. Current address: 843 Health Sciences Dr. 3032 Hewitt Hall Irvine CA 92617. (949) 824-1867. Fax (949) 824-2305.

Introduction

Aspergillus fumigatus causes severe pulmonary and disseminated infections in patients with compromised immune systems due to solid organ and bone marrow transplant, HIV/AIDS and genetic immunodeficiencies (1, 2). However, *Aspergillus* and *Fusarium* species are also major causes of corneal infections (keratitis), which occur in immune competent individuals and are a significant cause of blindness worldwide (3). Spores (conidia) enter the cornea through epithelial abrasions and germinate into filamentous hyphae. Neutrophils are the predominant cell type in early stage corneal ulcers and in murine models of fungal keratitis (4–6), where they play an essential role in regulating hyphal growth. Previously we reported that neutrophils combat hyphal growth in the cornea through reactive oxygen species (ROS)[2] and iron limitation, and that *A. fumigatus* possesses antioxidant and iron acquisition mechanisms to allow for survival (7, 8).

In addition to iron, zinc and manganese are also required for fungal growth, and an important immune defense strategy is based on sequestering these metals, termed nutritional immunity (9). Calprotectin (CP)[3] is a heterodimer of S100A8 and S100A9, members of the S100 family of calcium binding proteins, which exhibits anti-microbial effects on bacteria, fungi and protozoa through sequestration of zinc and manganese at two binding sites formed at the dimer interface (10–12). CP comprises ~40% of total protein in the neutrophil cytoplasm and is also produced and secreted by other myeloid and non-myeloid cells, including macrophages, epithelial cells and keratinocytes under inflammatory stimuli (13–15). Neutrophil CP is also reported to mediate intracellular activities, including NADPH oxidase activation and ROS production, and cytoskeletal rearrangement (16, 17).

In the current study, we identify an essential role for neutrophil CP in regulating growth of the hyphal stage of *Aspergillus in vitro* and in a murine model of fungal keratitis. We also show CP-dependent chelation of both zinc and manganese is required to compete with the *A. fumigatus* ZafA-regulated zinc transporter system. In marked contrast, using fluorescent *Aspergillus* reporter (FLARE) conidia that simultaneously report phagocytic uptake and fungal viability (18), we found no role for CP in neutrophil killing of the conidia stage of *A. fumigatus* either *in vitro* or in a murine pulmonary challenge model with conidia.

Together, these observations identify a stage - specific role for neutrophil CP in combatting *A. fumigatus* infections. Given the importance of this pathogen as a cause of severe pulmonary, systemic and corneal disease, these findings may lead to development of more targeted therapies for these infections.

Materials and Methods

Mouse Strains

All animals were used in accordance with the guidelines of the CWRU Institutional Animal Care and Use Committee (IACUC) and the MSKCC IACUC. S100A9$^{-/-}$ mice were

[2]ROS (Reactive Oxygen Species)
[3]CP (Calprotectin, S100A8/A9 heterodimer)

provided by Paul Fidel (LSU, Baton Rouge, LA). $CD18^{-/-}$ mice were originally provided by Claire Doerschuk (UNC, Chapel Hill, NC). Age and sex matched C57BL/6 mice were purchased from Jackson Laboratories (Bar Harbor, ME). For pulmonary challenge experiments, S100A9 and WT BM chimeric mice were generated by reconstituting lethally irradiated (9.5 Gy) recipients (C57BL/6.SJL mice) with 2–5 × 10^6 $S100A9^{(-/-)}$ or C57BL/6 BM cells and resting them for 6–8 weeks prior to use in experiments. Enrofloxacin treatment for 14 days in drinking water was given to prevent bacterial infections. Animal studies were compliant with all applicable provisions established by the Animal Welfare Act and the Public Health Services Policy on the Humane Care and Use of Laboratory Animals.

Fungal Strains and Growth Conditions

Strains used in this study are identified in Table I. Strains were grown on Sabouraud Dextrose Agar (SDA) (dsRed strains) or Vogel's minimal medium (VMM) + 2% agar +/− 0.5 mM $ZnSO_4$ (for Zn-deficient strains). Strains were grown at 37 °C for 3–5 days for sporulation and conidia were isolated by disruption in PBS and filtration through sterile cotton gauze.

Mouse Model of Fungal Keratitis

Mice were anesthetized and the corneal epithelium was penetrated with a 30G needle and 2 μl of conidial suspension (25,000 conidia/μl PBS) was injected into the corneal stroma with a 33G Hamilton syringe. Mice were imaged under a stereomicroscope at 24–48 hours pi. Whole eyes were homogenized in sterile PBS in a Mixer Mill MM300 (Retsch). Serial dilutions were plated in SDA (dsRed strains) or VMM + 2% agar +/− 0.5 mM $ZnSO_4$ (Zn-deficient strains) and incubated 24h at 37 °C. CFU was counted after 24h. dsRed expressing *A. fumigatus* eyes were imaged at 24–48h post-infection and opacity (pixel intensity) and integrated intensity of fluorescence was quantified using Metamorph software as described (5).

In some experiments, recombinant calprotectin or PBS (10μl) was injected into the sub-conjunctival space at the time of infection.

Murine Conidia Pulmonary Challenge Model

Intratracheal infections were performed as described earlier (18). Briefly, a blunt 20G needle was used to deliver conidia into the trachea of anesthetized mice. BAL and lung tissues were processed for flow cytometry as previously described (19). Briefly, single cell suspension of lungs and BAL cells were stained with the following Abs: anti-Ly6G (clone 1A8), anti-CD11b (clone M1/70), anti-CD45.1 (clone A20), anti-CD45.2 (clone 104), anti-Ly6B.2 (clone 7/4). Neutrophils were identified as $CD45^+CD11b^+Ly6C^{lo}Ly6G^+Ly6B.2^+$ cells. The data were collected on a BD LSR II flow cytometer and analyzed on FlowJo, version 9.7.6 (Treestar, Ashland, OR).

FLARE Conidia Preparation and *In Vitro* Assay

A. fumigatus strain 293 (AF293) was genetically modified to express dsRed and FLARE conidia were labeled as described previously (18). In all experiments, % uptake = ($dsRed^+AF633^+$ + dsRed−$AF633^+$/total) and % viability = ($dsRed^+AF633^+$/ $dsRed^+AF633^+$

+ dsRed−AF633^{+}). For *in vitro* experiments, FLARE conidia were added at MOI 2 to 1 × 10^6 peritoneal neutrophils in RPMI + 5% FBS for 8h at 37 °C. Cells were washed and re-suspended in FACS buffer. Data were collected on a BD Accuri C6 flow cytometer and analyzed on Accuri C6 and FlowJo software.

Isolation of Mouse Peritoneal Neutrophils

Mice were injected IP with 3% thioglycollate at 18h and 3h prior to euthanasia. The peritoneal cavity was lavaged with sterile PBS and neutrophils were purified by negative selection using an EasySep mouse neutrophil enrichment kit (StemCell, Vancouver, BC). Neutrophil purity of > 90% was verified by Wright-Geimsa staining. Neutrophils were re-suspended in RPMI 1640. To obtain neutrophil lysates, purified neutrophils at 2 × 10^6 cells/ml in RPMI 1640 were freeze-thawed at −80°C for 3 cycles. Lysates were spun at 10,000xg for 10 min and supernatants were collected.

Isolation of Human Neutrophils

Whole blood was collected from healthy donors between age 18–65 in accordance with the Declaration of Helsinki guidelines and the Institutional Review Board of the University of California Irvine. Red blood cells were separated in 3% Dextran (Sigma Aldrich, St. Louis, MO) PBS and neutrophils were purified from remaining cells by overlay on a Ficoll (GE Healthcare) density gradient and centrifugation at 500xg for 25 min. Remaining RBCs were lysed and neutrophils were re-suspended in RPMI 1640. Purity (>90%) was assessed by flow cytometry using anti-human CD16 and CD66b antibodies (eBioscience, San Diego, CA). Live/Dead fixable violet (Thermo Fisher) was used to gate live cells and positive populations were identified using FMO controls.

In Vitro Hyphal Growth Assays

Conidia (3,000 conidia/well) were grown in VMM +/− $ZnSO_4$ (Zn-deficient strains) for 6h to hyphal stage. Hyphae were washed 2X in PBS. Live neutrophils, lysates or recombinant CP in RPMI were incubated with hyphae for 16h at 37 °C. For some experiments $ZnSO_4$ (Sigma Aldrich 83265) or $MnSO_4$ (Sigma Aldrich M7899, St. Louis, MO) was added to media. Hyphae were stained with 50 μl Caclofluor white stain (undiluted)/well (Sigma Aldrich 18909) and washed 3X in ddH_20. Fluorescence at 360/440 nM was assessed using a Synergy HT plate reader (Biotek, Winooski, VT). % Fungal mass is calculated as a as percent of total hyphae when grown in RPMI media alone (experimental/control × 100).

Histology and Immunohistochemistry

Whole eyes were fixed in 10% phosphate buffered formalin, paraffin embedded and sectioned. PASH and GMS staining were performed by the CWRU Visual Science Research Center histology core. For immunohistochemistry, sections were treated with proteinase K (Dako 2015-011, Carpinteria, CA) and blocked in 1.5% serum. Mouse S100A9 polyclonal Ab (2 μg/ml, R&D Systems AF2065, Minneapolis, MN), Mouse S100A8 polyclonal Ab (2 μg/ml R&D Systems AF3059), or Anti-mouse neutrophil antibody NIMP-R14 (20 μg/ml) were used, followed by staining with Alexafluor 488 Chicken anti-goat IgG (1:2000, Life Technologies A2467, Grand Island, NY) or Alexafluor 488 Goat anti-rat IgG (1:250, Life

Technologies A11006). Slides were imaged at 200–400X. Neutrophil quantification from histological sections was obtained by measuring % NIMP-R14 positive area/cornea using Metamorph software.

Flow Cytometry of Cornea Cell Suspensions

Corneas were dissected at 24–48h pi and treated with 1X collagenase for 1–2 h. Cell suspensions were washed in 1X PBS + 5% FBS, incubated with anti-mouse CD16/CD32 (clone 93, eBioscience 16–0161-86, San Diego, CA)(to block Fc receptors) and stained with anti-mouse neutrophil antibody NIMP-R14-PE (abcam ab125259, Cambridge, MA) or isotype for 1h and live/dead fixable far read stain (Thermo Fisher). For intracellular staining, cells were fixed and permeabilized using an intracellular staining kit (eBioscience). Cells were incubated with Mouse S100A9 polyclonal Ab (R&D Systems AF2065), Mouse S100A8 polyclonal Ab (R&D Systems AF3059), or isotype for 45 min, washed and incubated with Alexafluor 488 Chicken anti-goat IgG (1:2000, Life Technologies A2467) for 30 min, washed, resuspended in FACS buffer and analyzed in a BD Accuri C6 (San Jose, CA). Analysis was performed using Accuri C6 software. Cells were gated on FSC/SSC, followed by live cells.

Cytokine and calprotectin quantification by ELISA

Corneas were dissected at 6–48h post-infection and homogenized in 150 μl 1X PBS using a Mixer Mill MM300 (Retsch) and lysates were analyzed for mS100A8 (R&D DY3059), mS100A9(R&D DY2065), mCXCL1/KC(R&D DY453), mCXCL2/MIP-2(R&D DY452) or mMPO(R&D DY3667), according the manufacturer instructions. For neutrophil lysates, purified C57BL/6 neutrophils at a concentration of 1×10^6/ml were lysed in 0.5% Triton X-100 in PBS and 10-fold serial dilutions were analyzed for mS100A8 and mS100A9.

Recombinant Calprotectin Methods

Recombinant human wild-type CP, and the CPΔZn/Mn and CPΔMn mutants, were expressed, purified and tested for activity as described previously (12).

Statistical Analysis

A Mann-Whitney U test was used for unpaired comparison of two groups for all *in vivo* and biological replicates. *In vitro* experiments are shown as one representative experiment with a minimum of three technical replicates per experiment and groups compared using the Student's t-test. Survival data was analyzed by long rank test. All statistical analyses were performed with GraphPad Prism software, v6.0c (La Jolla, CA). A p value < 0.05 was considered significant. (* $P \leq 0.05$, ** $P \leq 0.01$, *** $P \leq 0.001$)

Results

Neutrophil calprotectin regulates growth of *A. fumigatus* hyphae in the cornea

To evaluate the role of CP in regulating *A. fumigatus* hyphal growth, corneas of C57BL/6 and CP-deficient S100A9$^{-/-}$ mice were infected with *A. fumigatus* dsRed conidia, and hyphal growth was monitored at 24 and 48h post-infection (pi), which we reported is the

peak time of corneal inflammation and neutrophil infiltration (5). Fungal burden was measured by dsRed imaging and CFU.

S100A9$^{-/-}$ mice had elevated dsRed fluorescence at 24 and 48h and significantly elevated CFU at 48h compared to C57BL/6 (Fig 1A–C). Since CP is reported to mediate neutrophil chemotaxis (20), we examined whether S100A9$^{-/-}$ mice have impaired neutrophil recruitment during infection. Neutrophils from infected corneas were quantified by flow cytometry of corneal cell suspensions, IHC in corneal sections and myeloperoxidase (MPO) ELISA on corneal lysates. There was no significant difference in neutrophil numbers between C57BL/6 and S100A9$^{-/-}$ (Fig 1D and S1C–D), indicating that the increased hyphal burden in S100A9$^{-/-}$ mice is not due to impaired neutrophil migration. We also measured corneal opacity as an indicator of inflammation, and found no significant difference between S100A9$^{-/-}$ and C57BL/6 mice (Fig S1A–B). Furthermore, infected corneas of C57BL/6 and S100A9$^{-/-}$ mice had comparable levels of the neutrophil chemokines CXCL1 and CXCL2 (Fig S1E–F), which are essential for neutrophil chemotaxis in pulmonary and cornea infection models (5, 21).

To determine whether neutrophils are the source of CP during infection, adjacent corneal sections were immunostained with NIMP-R14, or with S100A8 and S100A9 antibodies. S100A8 and S100A9 staining increased from 24 to 48 h and coincided with NIMP-R14 staining (Fig 1E). Neutrophils, but not S100A8 or S100A9 were detected in corneal sections or single cell suspension from infected S100A9$^{-/-}$ mice (Fig S1G, H), which is consistent with previous reports that S100A8 is not expressed in the absence of S100A9 (22). Although S100A8 and S100A9 are also produced by epithelial cells (15), we did not detect S100A8 or S100A9 in the corneal epithelium. Total S100A8 and S100A9 proteins in infected corneas were quantified by ELISA and found to be elevated at 6, 24 and 48h post-infection compared with naïve C57BL/6 mice (Fig 1F). As an additional indicator that infiltrating myeloid cells rather than resident epithelial cells are the source of S100A8 and S100A9 in infected corneas, we infected corneas of CD18$^{-/-}$ mice, which lack the β2 subunit of CD11/CD18 integrin required for neutrophil trans-endothelial migration to the cornea, and found significantly lower levels of both proteins (Figs 1F and S1G) (8).

As an additional approach to determine if neutrophils are the primary source of S100A8 and S100A9, corneal cell suspensions were stained for intracellular S100A8 and S100A9 and cell surface NIMP-R14 and examined by flow cytometry. We found that >90% S100A8+ and S100A9+ cells were also NIMP-R14+ (Fig 1G, S1H).

Finally, to determine whether exogenous CP could impair hyphal growth during infection, S100A9$^{-/-}$ mouse corneas were infected with *A. fumigatus*-dsRed, and 1 μg total recombinant CP was administered into the sub-conjunctival space simultaneously where it will diffuse into the corneal stroma. Fig 1H–I shows that mice administered CP had significantly less hyphal mass than those given vehicle only, as measured by dsRed fluorescence, indicating that CP has a direct protective effect during *A. fumigatus* corneal infection.

Collectively, these data indicate that neutrophil-derived CP has an essential role in regulating *A. fumigatus* infection in the cornea.

Neutrophil calprotectin regulates growth of *A. fumigatus* hyphae *in vitro*

To determine if neutrophil CP directly limits *A. fumigatus* hyphal growth, peritoneal neutrophils from C57BL/6 and S100A9$^{-/-}$ mice were incubated with *A. fumigatus* hyphae. Fungal mass was measured following staining with calcofluor white, which binds cell wall chitin and can be quantified by fluorimetry (8). We found that 2×10^5 live neutrophils was the minimum number that significantly inhibited fungal growth in vitro (Figure S1I), although lysates from 1×10^5 neutrophils also significantly inhibited fungal growth (Figure S1J), the difference likely a consequence of only partial CP release from live neutrophils. We also quantified S100A8 and S100A9 in neutrophil lysates by ELISA, and found that murine neutrophils contained ~0.076 pg/cell (Fig. S1K).

Hyphae grown in medium alone exhibited normal branching morphology; however in the presence of C57BL/6 neutrophils, hyphal morphology was distinct, with short hyphal filaments and increased branching (Fig 2A). In contrast, hyphae incubated with S100A9$^{-/-}$ neutrophils resemble hyphae grown in RPMI alone (Fig 2A), indicating a direct effect of CP on growing hyphae. Calcofluor quantification revealed significantly higher fungal mass when incubated with S100A9$^{-/-}$ compared to C57BL/6 neutrophils (Fig 2B, Fig S1I). S100A8/A9 is reported to mediate production of reactive oxygen species (ROS) through NADPH oxidase, which is the dominant source of ROS and requires live cells (17),(8). Therefore, to determine if there is a contributing role for ROS in CP – mediated hyphal killing, neutrophils were lysed and incubated with hyphae. We found that similar to live neutrophils, there was significantly higher fungal mass when hyphae were incubated with S100A9$^{-/-}$ compared to C57BL/6 neutrophil lysates (Fig 2C), indicating that ROS is not required for neutrophil CP activity.

Taken together with the *in vivo* studies, these data indicate that neutrophils have a non-redundant role in controlling *A. fumigatus* infection through CP-mediated inhibition of hyphal growth.

Calprotectin zinc and manganese chelation contribute to anti-fungal activity

To examine the direct effect of CP on *A. fumigatus* hyphal growth *in vitro* and to assess the relative contribution of Zn and Mn chelation in CP activity, wild-type *A. fumigatus* hyphae were incubated with recombinant CP in the presence of 1μM or 5μM $MnSO_4$ and increasing concentrations of $ZnSO_4$.

Hyphae incubated with 25μg/ml recombinant CP exhibited the short hyphal filaments and increased branching shown above in the presence of C57BL/6 neutrophils (Figs 3A and 2A). To determine if hyphal growth can be rescued by Zn or Mn, we measured *A. fumigatus* hyphal growth following incubation with CP in the presence of $ZnSO_4$ and $MnSO_4$. We found that hyphal mass in the presence of 50 μg/ml (~1.4μM) CP was significantly lower than hyphae grown in RPMI alone (Fig 3B). As 1 mole of CP can bind either 2 moles of Zn or 1 mole of Zn plus 1 mole of Mn (12), rescue of *A. fumigatus* hyphal growth to 100% was

found to require > 2 μM $ZnSO_4$, whereas 2μM $ZnSO_4$ was sufficient to rescue in the presence of 1μM or 5μM $MnSO_4$. Conversely, an excess (5μM) of Mn alone only partially rescued growth (Fig 3B), which is likely due to Mn occupying only one of the two CP binding sites.

As a complementary approach to determine the relative contribution of Zn and Mn, we performed experiments with recombinant CP mutants with altered binding sites to either Mn alone or Zn and Mn (12): CPΔMn, lacking high affinity binding of Mn but with completely normal binding of Zn, and CPΔZn/Mn, lacking high affinity binding of both Zn and Mn. Fig 3C shows that whereas hyphal mass in the presence of wild-type CP was approximately 10% of growth in medium alone, hyphal mass in the presence of CPΔMn was significantly higher, though still inhibitory, In contrast, hyphal growth was unimpaired in the presence of the CPΔZn/Mn mutant, indicating complete loss of anti-fungal activity (Fig 3D).

Finally, to demonstrate that neutrophil anti-fungal activity depends on metal chelation, 2×10^5 purified human neutrophils were incubated with wild-type *A. fumigatus* hyphae in vitro +/− $ZnSO_4$ or $MnSO_4$ and fungal growth was measured. Neutrophils inhibited fungal growth more than 95%, which was reversed in the presence of $ZnSO_4$ (5 μM), but not when $MnSO_4$ (5 μM) was added (Fig 3E–F).

ZafA mediated zinc uptake contributes to *A. fumigatus* virulence during corneal infection and resistance to calprotectin

A. fumigatus expresses the zinc sensitive transcription factor ZafA under Zn limiting conditions, which up-regulates the expression of the zinc transporters ZrfA, ZrfB and ZrfC and the putative zinc binding protein Aspf2 (23–25). To determine whether ZafA mediated zinc uptake is necessary to compete with calprotectin, parent strain (WT) and Δ*zafA* mutant *A. fumigatus* hyphae were incubated with a 5×10^4 C57BL/6 or $S100A9^{-/-}$ neutrophils or with recombinant CP, and hyphal growth was measured following calcofluor staining.

This low number of C57BL/6 neutrophils did not inhibit growth of the WT *A. fumigatus* hyphae; however, growth of Δ*zafA* hyphae was significantly lower (Fig 4A), indicating increased sensitivity of this mutant. In contrast growth of Δ*zafA* mutants was not inhibited when incubated with the same number of $S100A9^{-/-}$ neutrophils (Fig 4A). Consistent with these data, growth of the Δ*zafA* mutant was significantly less than WT when incubated with recombinant CP (Fig 4B), indicating that ZafA is required for optimal growth in the presence of CP.

To determine if ZafA is required for growth in the cornea, C57BL/6 mice were infected with WT or Δ*zafA* mutant conidia, and CFU/eye were assayed after 48h. Corneas infected with Δ*zafA* had less hyphae in the corneal stroma than those infected with WT, as detected by GMS staining (Fig 4C), and significantly lower CFU than WT (Fig 4D). There was no significant difference in the number of neutrophils in the corneas of mice infected with WT vs. Δ*zafA A. fumigatus* when quantified by NIMP-R14 reactivity of corneal sections and image analysis (Fig 4E–F). Growth of Δ*zrfC*, Δ*zrfAB* and Δ*aspf2 A. fumigatus* in the cornea was not significantly different from the WT (Fig S2D–F). Further, although there was less

CFU in a Δ*zrfABC* mutant, this strain also did not grow as well as the WT or Δ*zafA in vitro* (Fig S2A–C).

Together, these data indicate that ZafA protein is essential for virulence during corneal infection and ZafA mediated zinc uptake competes with CP mediated zinc sequestration.

Calprotectin is not required for conidial phagocytosis and killing

In addition to metal chelation, S100A8 and S100A9 have been shown to promote neutrophil phagocytosis and intracellular killing of bacteria by ROS (26). Therefore to determine if CP contributes to neutrophil phagocytosis and conidial killing *in vitro*, peritoneal neutrophils from C57BL/6 or S100A9$^{-/-}$ mice were incubated with fluorescent *Aspergillus* reporter (FLARE) conidia as described (18). FLARE conidia express dsRed protein, which acts as an indicator of live conidia and is extinguished upon loss of conidial viability. FLARE conidia also incorporate Alexa Fluor 633 extracellularly, which persists even after loss of conidial viability (18). Thus, FLARE conidia can be harnessed to monitor conidial uptake and viability during cellular encounters with phagocytes, since phagocytes that contain live (DsRed+ Alexa Fluor 633+) conidia can be distinguished from counterparts that contain killed (DsRed- Alexa Fluor 633+) conidia) (18, 27). Representative images of neutrophils containing live or dead FLARE conidia, or bystander neutrophils, are shown in Fig S3A.

Neutrophils were incubated with FLARE conidia for 8h, and the total and viable conidia were quantified by flow cytometry. There was no significant difference in either conidial uptake or viability between C57BL/6 and S100A9$^{-/-}$ neutrophils (Fig 5A–B), indicating that CP is not required for intracellular conidial killing *in vitro*.

To examine whether CP expression in hematopoietic cells is required for host defense against respiratory *A. fumigatus* pulmonary infection, we generated CD45.2^{+} S100A9$^{-/-}$ → C57BL/6.SJL bone marrow chimeric mice, together with CD45.2^{+} S100A9$^{+/+}$ → C57BL/6.SJL controls. Both groups of chimeric mice were infected with FLARE conidia by the intratracheal route, and at 12h pi, single cell suspensions from bronchoalveolar lavage fluid (BALF) and the lung were assessed for conidial uptake and killing. Conidial phagocytosis and viability was indistinguishable between S100A9$^{-/-}$ neutrophils and control neutrophils (Fig 5C–D). In addition, total S100A9$^{-/-}$ and S100A9$^{+/+}$ neutrophil counts were similar in both groups (Fig 5E), and mice that lack S100A9 in hematopoietic cells did not succumb to infection (Fig S3B).

Thus, CP expression in radiosensitive hematopoietic cells, including neutrophils, is dispensable for host defense against *A. fumigatus* conidia. Collectively, these data demonstrate that CP acts in a fungal stage-specific manner to restrict extracellular *A. fumigatus* hyphal growth and is dispensable for intracellular conidial killing.

Discussion

Nutritional immunity is an emerging concept that addresses the importance of nutrient regulation by the immune system as a means of controlling pathogen growth and survival (28, 29). Essential nutrients required by pathogens include amino acids, lipids and transition

metals such as iron, zinc, manganese and copper. For example, iron is an essential cofactor for many cellular processes(30), and we reported that neutrophils regulate *A. fumigatus* hyphal growth by sequestering iron, and that treating infected corneas with iron-binding protein lactoferrin or inhibiting *A. fumigatus* iron-binding siderophore synthesis with HMG-CoA reductase inhibitors (statins) reduced fungal burden (7). In the current study we extend our understanding of nutritional immunity in *A. fumigatus* infection to include a role for neutrophil calprotectin.

CP is an abundant cytosolic protein in neutrophils(13), and we found that neutrophils are the primary source of CP during infection of the cornea. Previous work has shown that neutrophils are essential for control of *A. fumigatus* keratitis in mice (8). We did not observe S100A8/A9 staining in corneal epithelium, despite a report of epithelial S100A8/A9 production in a *Pseudomonas* keratitis model (31). A study in the lung also showed that leucopenic mice had very low CP expression, indicating that neutrophils are the primary source of CP in *Aspergillus* infection (32). The high levels of S100A8 and S100A9 protein in infected corneas is consistent with reports that calprotectin can reach levels as high as 1 mg/ml in abscess fluid(10). The ELISA assay may in fact underestimated the concentration of CP in the tissue and in neutrophils due to the ability of S100A8 and S100A9 to form higher-order oligomers, which likely still have Zn and Mn chelating activity (33). We also demonstrated that CP is essential for control of *A. fumigatus* growth in the cornea but not in a conidia pulmonary challenge model. Further, we compared the ability of CP-deficient S100A9$^{-/-}$ neutrophils to inhibit hyphal growth with their ability to kill *A. fumigatus* conidia using fluorescent *Aspergillus* reporter (FLARE) conidia and found that whereas S100A9$^{-/-}$ neutrophils could not limit hyphal growth, there was no deficiency in their ability to kill intracellular conidia. This is in contrast to reports that S100A8/A9 may promote phagocytosis and ROS production in response to *E. coli* and zymosan (16, 26). Our findings describe CP as a specific regulator of extracellular *A. fumigatus* hyphal growth. Previous work identified neutrophil ROS and iron-chelating enzymes as essential in anti-fungal responses during keratitis (7, 8). Furthermore, neutrophils contain numerous anti-microbial peptides and enzymes including defensins, cathelicidin, proteases and chitinases, which potentially mediate killing and degradation of fungal pathogens (34, 35). Therefore CP likely inhibits growth early in infection, which complements other anti-fungal mechanisms.

Because the corneal stroma is avascular, infiltrating cells are recruited from limbal vessels in the peripheral cornea and migrate through the dense corneal stroma to the site of infection. Thus neutrophils do not reach the site of infection until hyphae are formed. In contrast, during *A. fumigatus* pulmonary infection neutrophils are rapidly recruited to the highly vascularized lung, and control the organisms through phagocytosis of conidia (19). Thus in the cornea, anti-hyphal responses are essential for control of infection.

These results also fit well with the recent finding that neutrophil extracellular traps (NETs) are generated specifically in response to large extracellular pathogens such as fungal hyphae (36). The anti-fungal activity of NETs has been attributed to CP in *Candida albicans* dermal abscess and intranasal infection models and in vitro in response *to Aspergillus nidulans* (37, 38). NETs have been identified in lungs of *A. fumigatus* infected mice (39, 40); however, rather than using resting conidia as used in the current study and which are the form that is

normally inhaled and phagocytosed, those reports instilled the lungs with conidia that had been previously incubated for 7h, or with hyphal fragments. Although we are investigating NET formation during fungal corneal infection, those studies and ours indicate that CP, and therefore CP-laden NETs, are important to regulate growth of extracellular hyphae rather than conidia. However, Urban et al. demonstrate only ~30% of CP was contained within NETs while the remainder is found in the supernatant or associated with cellular remnants (37). This suggests the possibility of NET-independent secretion of CP. In activated monocytes S100A8 and S100A9 proteins were shown to be released in a non-classical, energy-dependent manner by associating with microtubules (41). Further studies on CP release by neutrophils and other cell types are warranted.

Several properties have been reported for CP, including direct chemotactic activity and chemoattractant response in neutrophils (20, 42). However, we found no difference in the number of neutrophils recruited to infected corneas of S100A9$^{-/-}$ mice or in S100A9$^{-/-}$ neutrophil migration to lungs, and no significant difference in corneal opacity between C57BL/6 and S100A9 −/− mice. This observation is consistent with a recent report demonstrating that although S100A8/A9 can induce neutrophil chemotaxis, its absence does not affect neutrophil recruitment *in vivo* in a murine model of vaginal candidiasis (15). Further, calprotectin is reported to promote phagosomal ROS production in response to zymosan particles or *E. coli* (16, 26); however, we found no impairment of S100A9$^{-/-}$ neutrophils in the phagocytosis or cytotoxic activity against conidia. In contrast, lung neutrophils that are defective in NADPH oxidase activity show a defect in conidial killing when mice are infected intratracheally with the FLARE conidia (18). In the current study, regulation of hyphal growth by calprotectin does not require NADPH oxidase, as our findings with live neutrophils were replicated using neutrophil lysates. Therefore, CP appears to have no role in either neutrophil recruitment or in ROS production.

Instead, we show that CP anti-fungal activity depends on binding of Zn and Mn. Addition of Zn or Zn and Mn was found to reverse CP mediated *Aspergillus* anti-fungal activity *in vitro* (32). The current study extends these findings using CP mutants that lack the ability to bind either Zn and Mn or just Mn to show the relative contribution of each of these transition metals. We found that a CPΔZn/Mn mutant had no anti-fungal activity, whereas a CPΔMn mutant had only partial loss of activity. Furthermore, Zn alone rescued fungal growth in the presence of CP or human neutrophils, whereas Mn alone did not. These data indicate that Zn chelation is essential for anti-fungal activity, whereas Mn has only a minor contributing role. This is in contrast to bacteria, in which Mn binding has a significant role in the anti-microbial activity of CP (12, 43). CP-mediated Mn chelation has been shown to inhibit superoxide dismutase activity and reduce the virulence of *Staphylococcus aureus* (44). Zn is required for the function of numerous enzymes and transcription factors in *A. fumigatus*, whereas Mn function is not well characterized, although it is required for superoxide dismutase function (45).

A. fumigatus growth requires a Zn uptake system comprising the Zn-sensitive transcription factor ZafA, which is required for expression of zinc transporters ZrfA, ZrfB and ZrfC, and the putative Zn binding protein Aspf2 (23–25, 32). ZafA and ZrfC are required for virulence in a pulmonary aspergillosis model in which mice were immunosuppressed (24, 32). This

zinc transporter system is also important in *C. albicans* and *Cryptococcus gatti*, where it is required for yeast survival *in vivo* (46, 47). In the current study, we show that ZafA is also essential for virulence during corneal infection and that ZafA-deficient *A. fumigatus* strain has increased susceptibility to inhibition by neutrophils and CP. In contrast to pulmonary infection, we found no role for ZrfC *in vivo* during corneal infection. The difference between these and previous findings has yet to be determined; however, cornea has a higher Zn content that other tissues, including the lung and the blood (48); therefore ZrfA and ZrfB may compensate for ZrfC in this setting as ZrfA and ZrfB expression is elevated in the Δ*zrfC* mutant (32). A ZrfABC-deficient strain also demonstrated less virulence *in vivo* as well as significantly impaired growth *in vitro*. The difference in growth of this mutant compared to ZafA-deficient *A. fumigatus* may be due to low level constitutive (ZafA-independent) expression of Zrf transporters on the ZafA mutant, which are completely absent in ZrfABC-deficient strain (49). Due to its importance in both pulmonary and corneal infections, ZafA may be a target for anti-fungal therapies (50).

Although the *A. fumigatus* Zn transport system has been characterized, specific Mn transporters have yet to be identified in *A. fumigatus*. However, a recent report showed that *A. fumigatus* siderophores that bind iron can also bind Mn (51).

Although the zinc transport system is important in *A. fumigatus* survival in the lungs, our current findings using the fluorescent *Aspergillus* reporter (FLARE) viability assay showed that there was no significant difference in viable conidia in neutrophils from infected lungs of S100A9$^{-/-}$ bone marrow chimeric mice compared with C57BL/6 mice, which taken together with *in vitro* assays indicate that CP is not required for host survival in a pulmonary challenge model in which the immune system is otherwise intact. CP is likely also important in the immunosuppressed condition where hyphae are present as leucopenic mice have reduced CP expression in the lung and increased fungal burden (32), and patients who develop *Aspergillus* pulmonary infections are often either neutropenic or have neutrophil dysfunction (52).

Interestingly, there is also a CP – independent mechanism of zinc sequestration that targets intracellular pathogens. Macrophages can limit zinc uptake by fungal pathogen *Histoplasma capsulatum* by sequestering metals from the phagosome using the transporters *Slc30a4* and *Slc30a7* and metallothioneins (53). It is unclear whether this mechanism is relevant in *A. fumigatus* conidial killing in the phagosome, however, since conidia are dormant, whereas the yeast form of *H. capsulatum* is replicating, zinc sequestration may not influence conidia survival.

We found that recombinant human CP inhibited *Aspergillus* growth at concentrations as low as 6.25 μg/ml. In vitro assays with murine neutrophils required greater than 1×10^5 C57BL/6 neutrophils to inhibit growth similarly. Human neutrophils were found to contain an average of 25 pg CP per neutrophil(54), whereas we found that murine neutrophils contained only ~0.076 pg/cell. Importantly, although human and mouse S100A8 and S100A9 share 59% protein sequence identity, minimum inhibitory concentrations may differ. The high level of sequence identity and the fact that all metal ligand residues are identical suggest the Zn and Mn affinities are the same; however, dissociation constants

have only been measured for recombinant human CP (12). Furthermore, release of CP from live neutrophils is likely less than 100% and indeed, a lysate from 1×10^5 neutrophils effectively inhibited *Aspergillus* growth (37).

Treatment of *Aspergillus* infections is difficult due to a limited range of anti-fungal agents with variable efficacy and significant associated toxicity. We demonstrated that exogenous CP could control fungal growth in S100A9$^{-/-}$ mice. Therefore, treatment with CP could represent a therapeutic strategy for neutropenic patients with fungal infections. Overall, these studies suggest that inhibiting fungal Zn and Mn acquisition through chelators, such as calprotectin, or through new inhibitors of ZafA or other components Zn and Mn transport may represent a new therapeutic approach (50).

Supplementary Material

Refer to Web version on PubMed Central for supplementary material.

Acknowledgements

We thank the CWRU Visual Science Research Core, particularly Catherine Doller, Denice Major and Scott Howell, for excellent technical assistance. We thank Paul Fidel (LSU), for providing the S100A9$^{-/-}$ mice. TMH and AJ thank Karin Bornfeldt (UW) for the S100A9$^{-/-}$ bones used to make the chimaeras for the lung experiments.

References

1. Brown GD, Denning DW, Gow NA, Levitz SM, Netea MG, White TC. Hidden killers: human fungal infections. Sci Transl Med. 2012; 4 165rv113.
2. Miceli MH, Lee SA. Emerging moulds: epidemiological trends and antifungal resistance. Mycoses. 2011; 54:e666–e678. [PubMed: 21672045]
3. Thomas PA, Kaliamurthy J. Mycotic keratitis: epidemiology, diagnosis and management. Clinical microbiology and infection : the official publication of the European Society of Clinical Microbiology and Infectious Diseases. 2013; 19:210–220.
4. Karthikeyan RS, Leal SM Jr, Prajna NV, Dharmalingam K, Geiser DM, Pearlman E, Lalitha P. Expression of innate and adaptive immune mediators in human corneal tissue infected with Aspergillus or fusarium. The Journal of infectious diseases. 2011; 204:942–950. [PubMed: 21828275]
5. Leal SM Jr, Cowden S, Hsia YC, Ghannoum MA, Momany M, Pearlman E. Distinct roles for Dectin-1 and TLR4 in the pathogenesis of Aspergillus fumigatus keratitis. PLoS pathogens. 2010; 6:e1000976. [PubMed: 20617171]
6. Tarabishy AB, Aldabagh B, Sun Y, Imamura Y, Mukherjee PK, Lass JH, Ghannoum MA, Pearlman E. MyD88 regulation of Fusarium keratitis is dependent on TLR4 and IL-1R1 but not TLR2. Journal of immunology. 2008; 181:593–600.
7. Leal SM Jr, Roy S, Vareechon C, Carrion S, Clark H, Lopez-Berges MS, Di Pietro A, Schrettl M, Beckmann N, Redl B, Haas H, Pearlman E. Targeting iron acquisition blocks infection with the fungal pathogens Aspergillus fumigatus and Fusarium oxysporum. PLoS pathogens. 2013; 9:e1003436. [PubMed: 23853581]
8. Leal SM Jr, Vareechon C, Cowden S, Cobb BA, Latge JP, Momany M, Pearlman E. Fungal antioxidant pathways promote survival against neutrophils during infection. The Journal of clinical investigation. 2012; 122:2482–2498. [PubMed: 22706306]
9. Kehl-Fie TE, Skaar EP. Nutritional immunity beyond iron: a role for manganese and zinc. Current opinion in chemical biology. 2010; 14:218–224. [PubMed: 20015678]
10. Clohessy PA, Golden BE. Calprotectin-mediated zinc chelation as a biostatic mechanism in host defence. Scandinavian journal of immunology. 1995; 42:551–556. [PubMed: 7481561]

11. Sohnle PG, Hunter MJ, Hahn B, Chazin WJ. Zinc-reversible antimicrobial activity of recombinant calprotectin (migration inhibitory factor-related proteins 8 and 14). The Journal of infectious diseases. 2000; 182:1272–1275. [PubMed: 10979933]
12. Damo SM, Kehl-Fie TE, Sugitani N, Holt ME, Rathi S, Murphy WJ, Zhang Y, Betz C, Hench L, Fritz G, Skaar EP, Chazin WJ. Molecular basis for manganese sequestration by calprotectin and roles in the innate immune response to invading bacterial pathogens. Proceedings of the National Academy of Sciences of the United States of America. 2013; 110:3841–3846. [PubMed: 23431180]
13. Edgeworth J, Gorman M, Bennett R, Freemont P, Hogg N. Identification of p8,14 as a highly abundant heterodimeric calcium binding protein complex of myeloid cells. The Journal of biological chemistry. 1991; 266:7706–7713. [PubMed: 2019594]
14. Vogl T, Tenbrock K, Ludwig S, Leukert N, Ehrhardt C, van Zoelen MA, Nacken W, Foell D, van der Poll T, Sorg C, Roth J. Mrp8 and Mrp14 are endogenous activators of Toll-like receptor 4, promoting lethal, endotoxin-induced shock. Nature medicine. 2007; 13:1042–1049.
15. Yano J, Palmer GE, Eberle KE, Peters BM, Vogl T, McKenzie AN, Fidel PL Jr. Vaginal epithelial cell-derived S100 alarmins induced by Candida albicans via pattern recognition receptor interactions are sufficient but not necessary for the acute neutrophil response during experimental vaginal candidiasis. Infection and immunity. 2014; 82:783–792. [PubMed: 24478092]
16. Steinckwich N, Schenten V, Melchior C, Brechard S, Tschirhart EJ. An essential role of STIM1, Orai1, and S100A8-A9 proteins for Ca2+ signaling and FcgammaR-mediated phagosomal oxidative activity. Journal of immunology. 2011; 186:2182–2191.
17. Kerkhoff C, Nacken W, Benedyk M, Dagher MC, Sopalla C, Doussiere J. The arachidonic acid-binding protein S100A8/A9 promotes NADPH oxidase activation by interaction with p67phox and Rac-2. FASEB journal : official publication of the Federation of American Societies for Experimental Biology. 2005; 19:467–469. [PubMed: 15642721]
18. Jhingran A, Mar KB, Kumasaka DK, Knoblaugh SE, Ngo LY, Segal BH, Iwakura Y, Lowell CA, Hamerman JA, Lin X, Hohl TM. Tracing conidial fate and measuring host cell antifungal activity using a reporter of microbial viability in the lung. Cell reports. 2012; 2:1762–1773. [PubMed: 23200858]
19. Mircescu MM, Lipuma L, van Rooijen N, Pamer EG, Hohl TM. Essential role for neutrophils but not alveolar macrophages at early time points following Aspergillus fumigatus infection. The Journal of infectious diseases. 2009; 200:647–656. [PubMed: 19591573]
20. Ryckman C, Vandal K, Rouleau P, Talbot M, Tessier PA. Proinflammatory activities of S100: proteins S100A8, S100A9, and S100A8/A9 induce neutrophil chemotaxis and adhesion. Journal of immunology. 2003; 170:3233–3242.
21. Jhingran A, Kasahara S, Shepardson KM, Junecko BA, Heung LJ, Kumasaka DK, Knoblaugh SE, Lin X, Kazmierczak BI, Reinhart TA, Cramer RA, Hohl TM. Compartment-specific and sequential role of MyD88 and CARD9 in chemokine induction and innate defense during respiratory fungal infection. PLoS pathogens. 2015; 11:e1004589. [PubMed: 25621893]
22. Hobbs JA, May R, Tanousis K, McNeill E, Mathies M, Gebhardt C, Henderson R, Robinson MJ, Hogg N. Myeloid cell function in MRP-14 (S100A9) null mice. Molecular and cellular biology. 2003; 23:2564–2576. [PubMed: 12640137]
23. Amich J, Vicentefranqueira R, Leal F, Calera JA. Aspergillus fumigatus survival in alkaline and extreme zinc-limiting environments relies on the induction of a zinc homeostasis system encoded by the zrfC and aspf2 genes. Eukaryotic cell. 2010; 9:424–437. [PubMed: 20038606]
24. Moreno MA, Ibrahim-Granet O, Vicentefranqueira R, Amich J, Ave P, Leal F, Latge JP, Calera JA. The regulation of zinc homeostasis by the ZafA transcriptional activator is essential for Aspergillus fumigatus virulence. Molecular microbiology. 2007; 64:1182–1197. [PubMed: 17542914]
25. Vicentefranqueira R, Moreno MA, Leal F, Calera JA. The zrfA and zrfB genes of Aspergillus fumigatus encode the zinc transporter proteins of a zinc uptake system induced in an acid, zinc-depleted environment. Eukaryotic cell. 2005; 4:837–848. [PubMed: 15879518]
26. Simard JC, Simon MM, Tessier PA, Girard D. Damage-associated molecular pattern S100A9 increases bactericidal activity of human neutrophils by enhancing phagocytosis. Journal of immunology. 2011; 186:3622–3631.

27. Espinosa V, Jhingran A, Dutta O, Kasahara S, Donnelly R, Du P, Rosenfeld J, Leiner I, Chen CC, Ron Y, Hohl TM, Rivera A. Inflammatory monocytes orchestrate innate antifungal immunity in the lung. PLoS pathogens. 2014; 10:e1003940. [PubMed: 24586155]
28. Hood MI, Skaar EP. Nutritional immunity: transition metals at the pathogen-host interface. *Nature reviews* . Microbiology. 2012; 10:525–537. [PubMed: 22796883]
29. Zackular JP, Chazin WJ, Skaar EP. Nutritional Immunity: S100 Proteins at the Host-Pathogen Interface. The Journal of biological chemistry. 2015; 290:18991–18998. [PubMed: 26055713]
30. Cassat JE, Skaar EP. Iron in infection and immunity. Cell host & microbe. 2013; 13:509–519. [PubMed: 23684303]
31. Deng Q, Sun M, Yang K, Zhu M, Chen K, Yuan J, Wu M, Huang X. MRP8/14 enhances corneal susceptibility to Pseudomonas aeruginosa Infection by amplifying inflammatory responses. Investigative ophthalmology & visual science. 2013; 54:1227–1234. [PubMed: 23299480]
32. Amich J, Vicentefranqueira R, Mellado E, Ruiz-Carmuega A, Leal F, Calera JA. The ZrfC alkaline zinc transporter is required for Aspergillus fumigatus virulence and its growth in the presence of the Zn/Mn-chelating protein calprotectin. Cellular microbiology. 2014; 16:548–564. [PubMed: 24245710]
33. Vogl T, Gharibyan AL, Morozova-Roche LA. Pro-inflammatory S100A8 and S100A9 proteins: self-assembly into multifunctional native and amyloid complexes. International journal of molecular sciences. 2012; 13:2893–2917. [PubMed: 22489132]
34. van Eijk M, van Roomen CP, Renkema GH, Bussink AP, Andrews L, Blommaart EF, Sugar A, Verhoeven AJ, Boot RG, Aerts JM. Characterization of human phagocyte-derived chitotriosidase, a component of innate immunity. International immunology. 2005; 17:1505–1512. [PubMed: 16214810]
35. Kolar SS, Baidouri H, Hanlon S, McDermott AM. Protective role of murine beta-defensins 3 and 4 and cathelin-related antimicrobial peptide in Fusarium solani keratitis. Infection and immunity. 2013; 81:2669–2677. [PubMed: 23670560]
36. Branzk N, Lubojemska A, Hardison SE, Wang Q, Gutierrez MG, Brown GD, Papayannopoulos V. Neutrophils sense microbe size and selectively release neutrophil extracellular traps in response to large pathogens. Nature immunology. 2014; 15:1017–1025. [PubMed: 25217981]
37. Urban CF, Ermert D, Schmid M, Abu-Abed U, Goosmann C, Nacken W, Brinkmann V, Jungblut PR, Zychlinsky A. Neutrophil extracellular traps contain calprotectin, a cytosolic protein complex involved in host defense against Candida albicans. PLoS pathogens. 2009; 5:e1000639. [PubMed: 19876394]
38. Bianchi M, Niemiec MJ, Siler U, Urban CF, Reichenbach J. Restoration of anti-Aspergillus defense by neutrophil extracellular traps in human chronic granulomatous disease after gene therapy is calprotectin-dependent. The Journal of allergy and clinical immunology. 2011; 127:1243–1252. e1247. [PubMed: 21376380]
39. Rohm M, Grimm MJ, D'Auria AC, Almyroudis NG, Segal BH, Urban CF. NADPH oxidase promotes neutrophil extracellular trap formation in pulmonary aspergillosis. Infection and immunity. 2014; 82:1766–1777. [PubMed: 24549323]
40. Bruns S, Kniemeyer O, Hasenberg M, Aimanianda V, Nietzsche S, Thywissen A, Jeron A, Latge JP, Brakhage AA, Gunzer M. Production of extracellular traps against Aspergillus fumigatus in vitro and in infected lung tissue is dependent on invading neutrophils and influenced by hydrophobin RodA. PLoS pathogens. 2010; 6:e1000873. [PubMed: 20442864]
41. Rammes A, Roth J, Goebeler M, Klempt M, Hartmann M, Sorg C. Myeloid-related protein (MRP) 8 and MRP14, calcium-binding proteins of the S100 family, are secreted by activated monocytes via a novel, tubulin-dependent pathway. The Journal of biological chemistry. 1997; 272:9496–9502. [PubMed: 9083090]
42. McNeill E, Conway SJ, Roderick HL, Bootman MD, Hogg N. Defective chemoattractant-induced calcium signalling in S100A9 null neutrophils. Cell calcium. 2007; 41:107–121. [PubMed: 16814379]
43. Brophy MB, Nakashige TG, Gaillard A, Nolan EM. Contributions of the S100A9 C-terminal tail to high-affinity Mn(II) chelation by the host-defense protein human calprotectin. Journal of the American Chemical Society. 2013; 135:17804–17817. [PubMed: 24245608]

44. Kehl-Fie TE, Chitayat S, Hood MI, Damo S, Restrepo N, Garcia C, Munro KA, Chazin WJ, Skaar EP. Nutrient metal sequestration by calprotectin inhibits bacterial superoxide defense, enhancing neutrophil killing of Staphylococcus aureus. Cell host & microbe. 2011; 10:158–164. [PubMed: 21843872]
45. Lambou K, Lamarre C, Beau R, Dufour N, Latge JP. Functional analysis of the superoxide dismutase family in Aspergillus fumigatus. Molecular microbiology. 2010; 75:910–923. [PubMed: 20487287]
46. Citiulo F, Jacobsen ID, Miramon P, Schild L, Brunke S, Zipfel P, Brock M, Hube B, Wilson D. Candida albicans scavenges host zinc via Pra1 during endothelial invasion. PLoS pathogens. 2012; 8:e1002777. [PubMed: 22761575]
47. Schneider Rde O, Fogaca Nde S, Kmetzsch L, Schrank A, Vainstein MH, Staats CC. Zap1 regulates zinc homeostasis and modulates virulence in Cryptococcus gattii. PloS one. 2012; 7:e43773. [PubMed: 22916306]
48. Ugarte M, Grime GW, Osborne NN. Distribution of trace elements in the mammalian retina and cornea by use of particle-induced X-ray emission (PIXE): localisation of zinc does not correlate with that of metallothioneins. Metallomics : integrated biometal science. 2014; 6:274–278. [PubMed: 24226809]
49. Amich J, Calera JA. Zinc Acquisition: A Key Aspect in Aspergillus fumigatus Virulence. Mycopathologia. 2014
50. Vicentefranqueira R, Amich J, Laskaris P, Ibrahim-Granet O, Latge JP, Toledo H, Leal F, Calera JA. Targeting zinc homeostasis to combat Aspergillus fumigatus infections. Frontiers in microbiology. 2015; 6:160. [PubMed: 25774155]
51. Farkas E, Szabo O, Parajdi-Losonczi PL, Balla G, Pocsi I. Mn(II)/Mn(III) and Fe(III) binding capability of two Aspergillus fumigatus siderophores, desferricrocin and N', N'', N'''-triacetylfusarinine C. Journal of inorganic biochemistry. 2014; 139:30–37. [PubMed: 24959697]
52. Kosmidis C, Denning DW. Republished: The clinical spectrum of pulmonary aspergillosis. Postgraduate medical journal. 2015; 91:403–410. [PubMed: 26187954]
53. Subramanian Vignesh K, Landero Figueroa JA, Porollo A, Caruso JA, Deepe GS Jr. Granulocyte macrophage-colony stimulating factor induced Zn sequestration enhances macrophage superoxide and limits intracellular pathogen survival. Immunity. 2013; 39:697–710. [PubMed: 24138881]
54. Fagerhol MK, Nielsen HG, Vetlesen A, Sandvik K, Lyberg T. Increase in plasma calprotectin during long-distance running. Scandinavian journal of clinical and laboratory investigation. 2005; 65:211–220. [PubMed: 16095050]

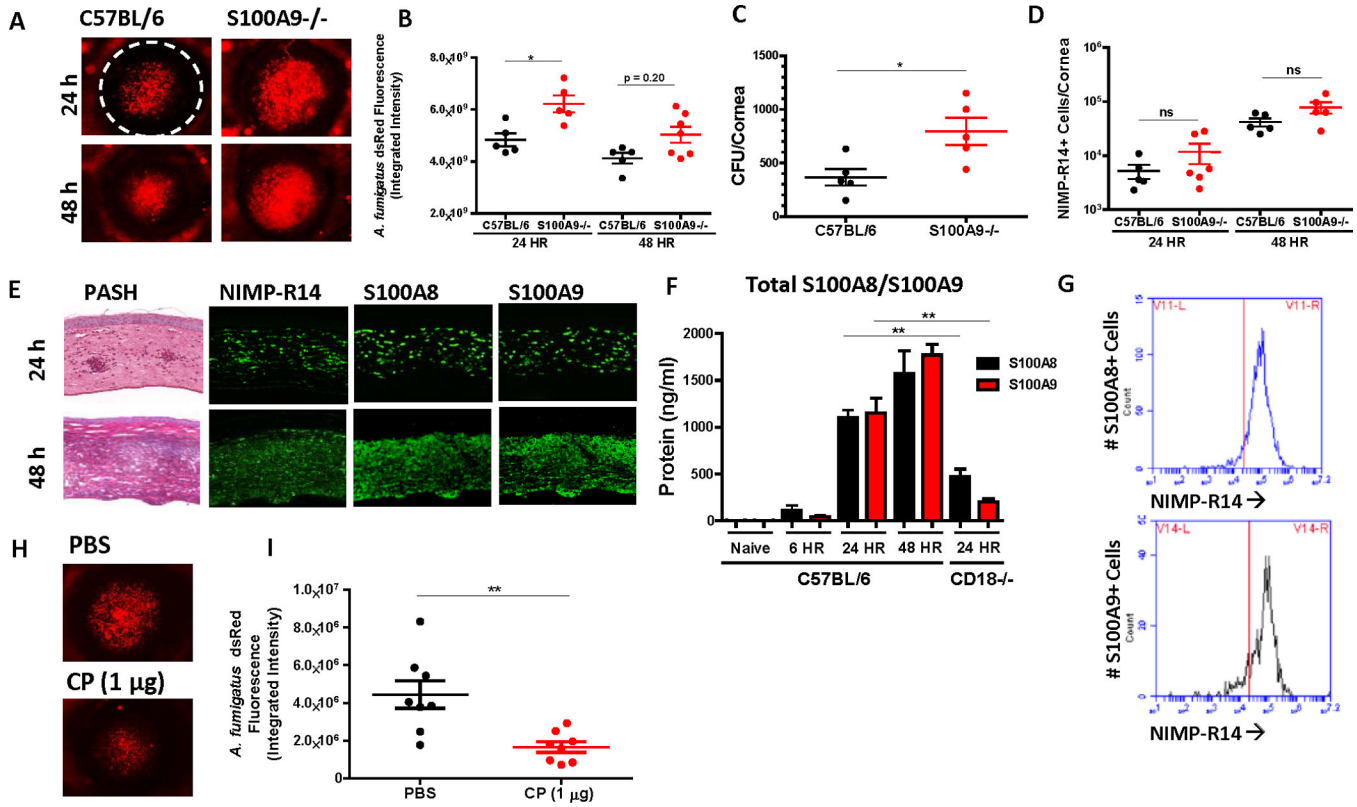

Figure 1. Effect of neutrophil calprotectin on *A. fumigatus* corneal infection

A. C57BL/6 or S100A9$^{-/-}$ mice were infected intrastromally with 50,000 *A. fumigatus* dsRed conidia **(A-D)** and corneas were imaged at 24 and 48h pi. **B**. Fungal burden measured by dsRed fluorimetry at 24 and 48h pi. **C**. CFU from whole eye homogenates measured at 48h pi. **D**. Neutrophil number in infected corneas measured as total NIMP-R14+ cells in corneal cell suspensions at 24 and 48h pi by flow cytometry. **E**. PASH and IHC for neutrophils (NIMP-R14), S100A8 and S100A9 in adjacent corneal sections from *A. fumigatus* infected C57BL/6 mice at 24 and 48h pi (400X). **F**. S100A8 and S100A9 expression by ELISA in naïve or *A. fumigatus* infected corneas of C57BL/6 or CD18$^{-/-}$ mice. **G**. NIMP-R14 staining in S100A8 and S100A9-positive cells from *A. fumigatus* infected corneas of C57BL/6 mice at 24h pi. **H-I**. S100A9$^{-/-}$ mice were infected intrastromally with 50,000 *A. fumigatus* dsRed conidia and PBS or recombinant calprotectin (1 µg) was injected subconjunctivally at the time of infection. **H**. Representative images of *A. fumigatus* dsRed in infected corneas at 24 hrs pi. **I**. Fungal burden measured by dsRed fluorimetry at 24h pi. Experiments were repeated three times with 3–5 mice per group, A Mann-Whitney U test was used to determine significance. All data show mean +/− SEM. See also Figure S1.

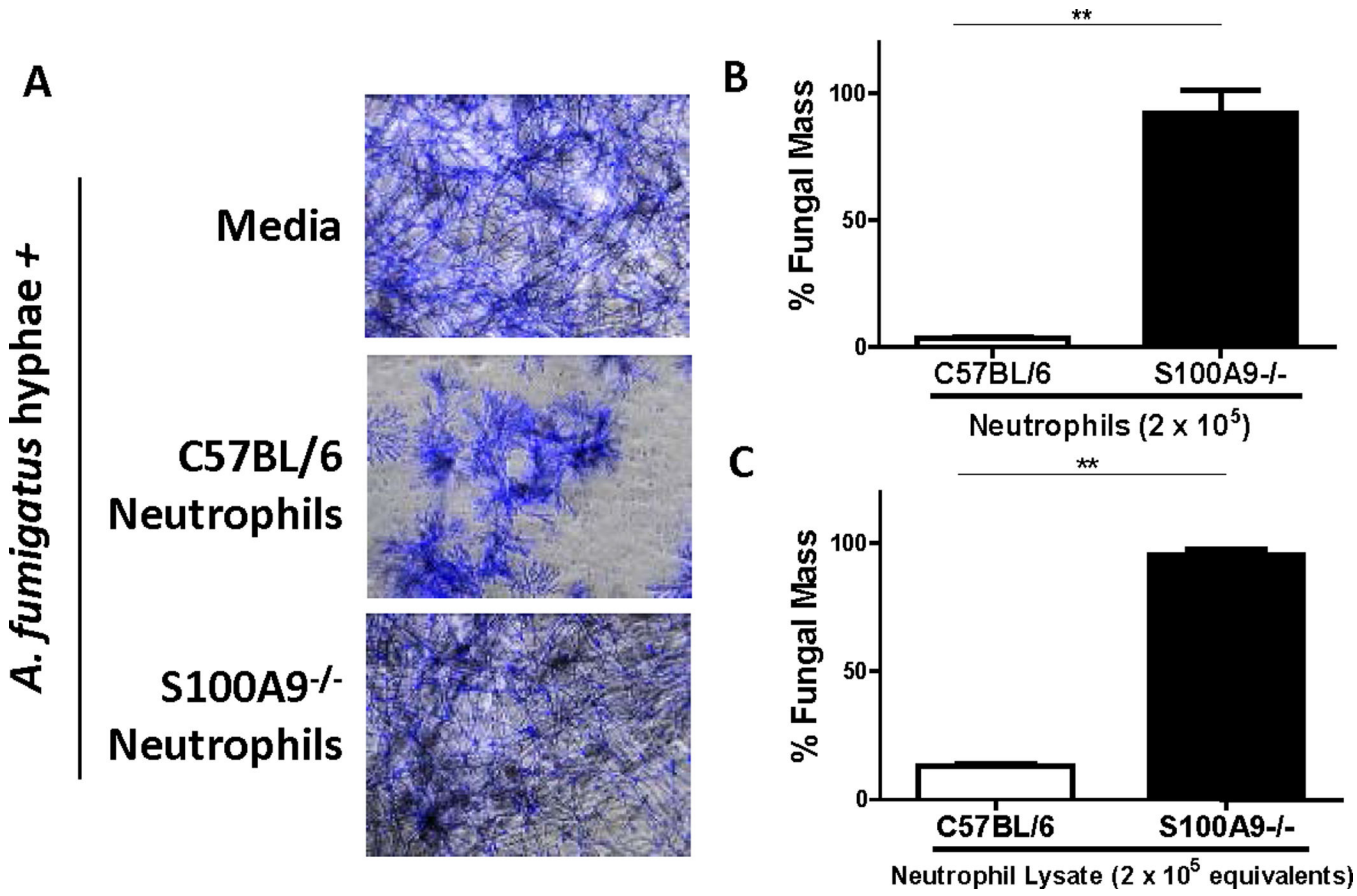

Figure 2. Effect of neutrophil calprotectin on *A. fumigatus* hyphal growth *in vitro*

Peritoneal neutrophils or neutrophil lysates from C57BL/6 or S100A9$^{-/-}$ mice were incubated 16h with *A. fumigatus* hyphae **(A-B)**, and hyphal growth was assessed by calcofluor staining **A**. Representative images of hyphae (200X); **B-C**. Quantification of hyphal growth in the presence of neutrophils or neutrophil lysates. % Fungal mass was calculated by fluorimetry of calcofluor and shown as percent of total hyphae when grown in media alone (experimental/control × 100). Representative *In vitro* experiments with 3–6 technical replicates per condition, significance was determined by student's t-test. All data show mean +/− SEM. See also Figure S1.

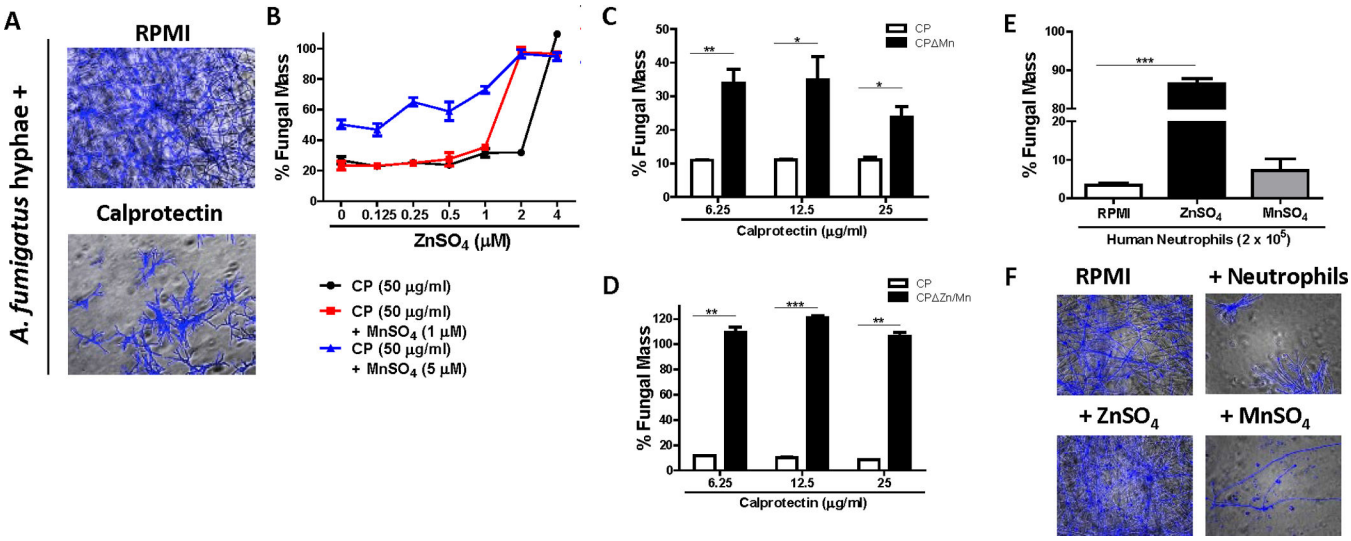

Figure 3. Zn and Mn binding contribute to calprotectin Anti *Aspergillus* activity

A. fumigatus hyphae were incubated +/− recombinant calprotectin for 16h and fungal growth was assessed by calcofluor staining **(A-D)**. % Fungal mass was calculated by fluorimetry of calcofluor and shown as percent of total hyphae when grown in media alone (experimental/control × 100). **A**. Representative images of hyphae (200X) in media +/− 25 μg/ml calprotectin **B**. Quantification of hyphael growth + 50 μg/ml calprotectin +/− increasing $ZnSO_4$ +/− 1 or 5 μM $MnSO_4$**C-D**. Quantification of hyphal growth of hyphae incubated with wild-type calprotectin (CP) vs. CPΔMn calprotectin (lacks Mn binding motif; note difference in the y axis scale) **(C)** or CP vs. or CPΔMn/Zn calprotectin (lacks Mn and Zn binding motifs). **E-F***A. fumigatus* hyphae were incubated with 2×10^5 human neutrophils in RPMI +/− 5 μM $ZnSO_4$ or $MnSO_4$ and fungal growth was assessed by calcofluor staining. **E**. % Fungal mass was calculated by fluorimetry of calcofluor and shown as percent of total hyphae when grown in media alone (experimental/control × 100). **F**. Representative images of hyphae (200X) in media +/− neutrophils, $ZnSO_4$ or $MnSO_4$. Representative *In vitro* experiments with 3–6 technical replicates per condition, significance was determined by student's t-test. Human neutrophils were tested from three separate donors.

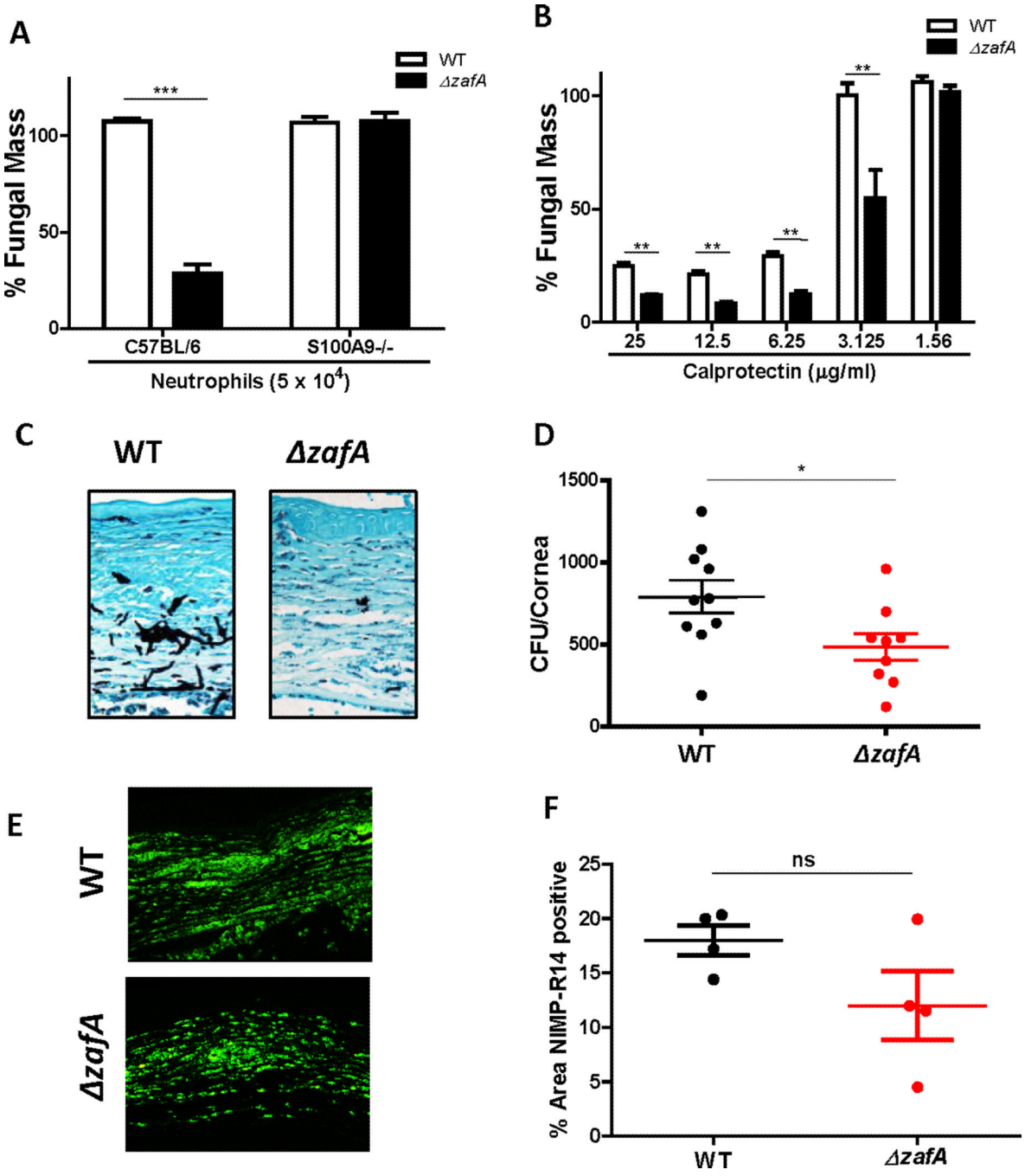

Figure 4. ZafA mediated zinc uptake in *A. fumigatus* virulence and susceptibility to calprotectin

WT or Δ*zafAA. fumigatus* hyphae were incubated with peritoneal neutrophils from C57BL/6 or S100A9−/− mice or recombinant calprotectin for 16h **(A-B)**. Fungal growth was assessed by calcofluor staining and % Fungal mass was calculated by fluorimetry of calcofluor and shown as percent of total hyphae when grown in media alone (experimental/control × 100). **A**. Growth of hyphae incubated with C57BL/6 or S100A9$^{-/-}$ neutrophils (0.5 × 10^5/well). **B**. Growth of hyphae incubated with increasing doses of CP. Representative *In vitro* experiments with 3–6 technical replicates per condition, significance was determined by

student's t-test. C57BL/6 mice were infected intrastromally with 50,000 WT or Δ*zafA A. fumigatus* conidia **(C-D). C**. Fungal growth assessed in infected corneal sections by GMS stain (hyphae appear black) at 48h pi (400X). **D**. CFU of WT vs. Δ*zafA* from whole eye homogenates measured at 48h pi. **E-F**. Neutrophil infiltration in C57BL/6 mice infected with WT or Δ*zafAA. fumigatus* assessed by IHC for NIMP-R14 in corneal sections and quantified using Metamorph (400x). *In vivo* experiment was repeated three times with at least 3 mice per group. Significance was assess by Mann-Whitney U test. All data show mean +/− SEM. See also Figure S2.

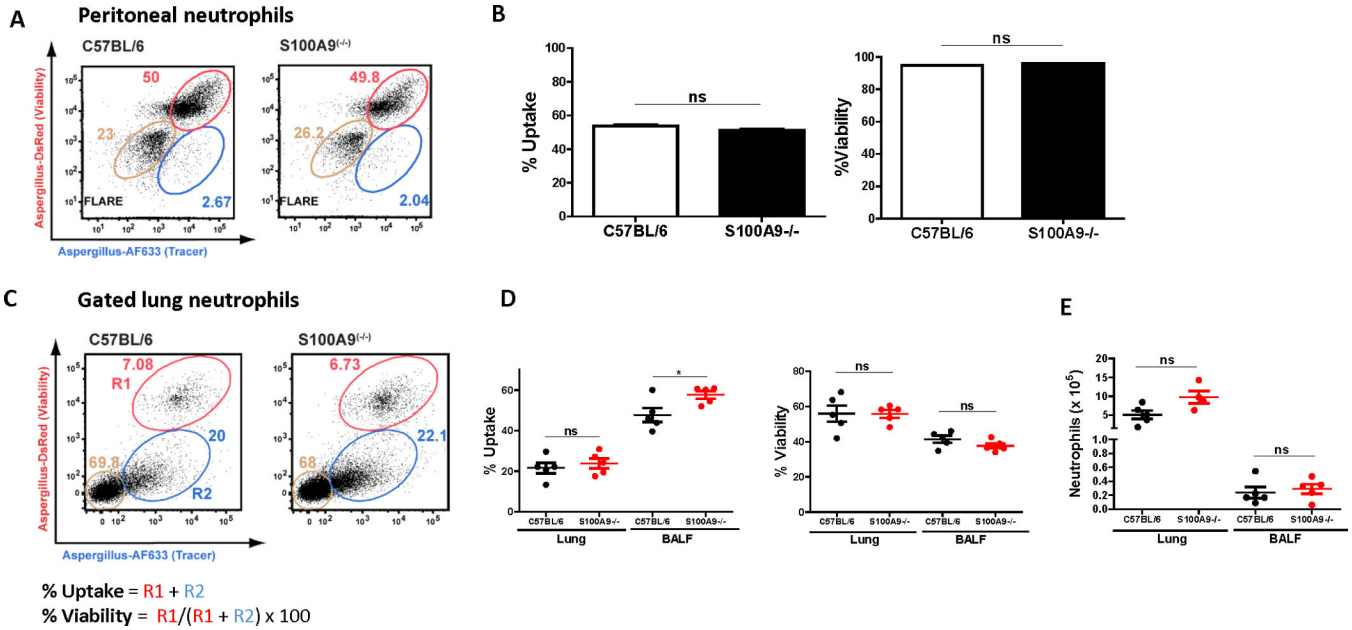

Figure 5. Conidia killing by neutrophils is independent of calprotectin

A. Representative dot plots of peritoneal C57BL/6 or S100A9$^{-/-}$ neutrophils incubated with FLARE (dsRed+ AF633+) conidia 8h. **B**. Uptake and viability of FLARE conidia incubated with C57BL/6 or S100A9−/− neutrophils *in vitro* for 8 hrs. Representative *In vitro* experiments with 3–6 technical replicates per condition, significance was determined by student's t-test. C57BL/6 or S100A9$^{-/-}$ bone marrow chimeras were challenged intratracheally with 3 × 10^7 FLARE conidia **(C-E). C**. Representative dot plots of neutrophils from lung and BALF analyzed for dsRed and AF633 fluorescence by flow cytometry. The tan gates indicate bystander neutrophils, and the red (R1) and blue (R2) gates indicate neutrophils that contain live or killed conidia, respectively. **D**. Uptake and viability of FLARE conidia in lung or BALF neutrophils 12h pi. **E**. Total neutrophils in lung or BALF 12h pi in C57BL/6 or S100A9$^{-/-}$ bone marrow chimeras. *In vivo* experiments were repeated twice with at least 3 mice per group. Significance was determined by Mann-Whitney U test. All data show mean +/− SEM. See also Figure S3.

Table I

Strains used in this study

Strain	Genotype	Phenotype	Reference
dsRed *A. fumigatus*	Af293.1: ΔpyrG1::gpdA::dsRed::pyrG	dsRed fluorescence	(5)
FLARE	Af293:pPgpd-dsRed	dsRed fluorescence (bright), labeled with AF633	(18)
WT/Parent Strain	WT	Wild-type	(24)
Δ*zafA*	Δ*zafA*	ZafA deficient	(24)
Δ*zrfABC*	Δ*zrfABC*	ZrfA, B, C deficient	(42)
Δ*zrfC*	Δ*zrfC*	ZrfC deficient	(23)
Δ*zrfAB*	Δ*zrfABC[zrfC]*	ZrfA, B deficient	(42)
Δ*asfp2*	Δ*aspf2*	Aspf2 deficient	(23)